Journal of Interfaces, Thin films, and Low dimensional systems 3 (2) Winter and Spring (2020) 297-304

The structure of $L1_0$-FePt nanoparticles in the presence of Ag

Scientific research paper

Mohammadreza Salahpour, Seyed Ali Sebt*, Ana Khajehnezhad

Department of physics, Science and Research Branch, Islamic Azad University, Tehran, Iran.

ARTICLE INFO

Article history:
Received 24 July 2020
Revised 27 November 2020
Accepted 19 December 2020
Available online 27 February 2021

Keywords:
$L1_0$-FePt nanoparticles
FePt-Ag
Orientation
Co-sputtering
RKKY interaction

ABSTRACT

Temperature above 600°C during the fabrication process is required to form the $L1_0$ compound ordering phase in FePt nanoparticles. The $L1_0$-FePt nanoparticles are ferromagnetic with high magnetic anisotropy. Practically, another ordering that is required is the orientation of their crystal c axis perpendicular to the plane of the nanolayer. The effects of the presence of Ag in reducing the transition temperature and making FePt nanocrystals in the $L1_0$-FePt phase aligned, in this work, have been studied and determined. The results of XRD analysis indicate that in fabrication using the co-sputtering method, firstly, the presence of Ag before annealing gives rise to the decline of the c parameter of the crystal lattice. This result of XRD analysis has been compared with the result of the RKKY exchange interaction model as an experimental confirmation of this model. Secondly, during annealing, with the formation of FePt-Ag nanostructure, the easy axis of FePt nanoparticles in the $L1_0$-FePt phase appears parallel to each other. These results, which are the consequence of the presence of Ag, are obtained by studying FE-SEM images, XRD patterns, and magnetic characterization.

1 Introduction

With paramagnetic elements of (Pd, Pt), the ordered alloys of Fe show $L1_0$-fct structure and ferromagnetic properties with high coercivity [1, 2]. The FePt alloys in the $L1_0$ phase have high coercivity and large uniaxial magnetocrystalline anisotropy energy density ($K_u \sim 7 \times 10^6$ J/m^3) [3, 4]. The magnetic properties of ordered $L1_0$-FePt alloys are determined by both direct Fe-Fe interactions between a Fe atom and its nearest neighbors in the Fe layer and polarization due to the indirect Fe-Pt-Fe interactions [5]. It can be possible that a nonferromagnetic ion separates two magnetic ions. There is another exchange interaction between the magnetic ions, which is called indirect exchange interaction, in which they can have a magnetic interaction mediated by the conduction electrons in their common nonferromagnetic neighbors [6].

*Corresponding author.
Email address: Sa.sebt@srbiau.iac.ir
DOI: 10.22051/jitl.2020.32375.1042

The coupling mechanism in Fe-Pt-Fe is the Ruderman-Kittle-Kasuya-Yosida (RKKY) interaction [7, 8]. This interaction can affect the coercivity and lattice constant of alloy [9]. The lattice constants, for example, of pure Fe and Pt are 2.87 Å and 3.92 Å, respectively. Nevertheless, the lattice constant of FePt alloy with fcc structure is a = 3.82 Å and for $L1_0$ -FePt structure, a and c parameters are 3.85 Å and 3.71 Å, respectively [10].

The FePt thin films deposited at room temperature (R.T.) have a chemical disordered fcc structure with soft magnetic properties, thus, to get hard magnetic properties with a chemical ordered structure ($L1_0$ phase), it is necessary for FePt thin films to deposit on a hot substrate or anneal after deposition at 600°C [11, 12] or higher [13]. So far, several methods were used to investigate this phase transition and control the nanostructure of the FePt [14, 15], such as the core-shell nanoparticles [16], the addition of a third element into FePt alloy, such as Cu [17- 20], Au [21, 22], Ni [23] and Mn [24, 25].

The impacts of adding Cu on FePt nanoparticles in references [18, 19] have been specified. The transition temperature of FePt to the $L1_0$ phase is reduced by Cu and the texture containing these nanoparticles is oriented, but it reduces the vertical magnetic anisotropy, so that in 9 and 15 atomic percentages of Cu and with annealing temperature of 600°C, the coercivity reaches less than half and nearly vanishes, respectively.

Ag addition to FePt films and Ag underlayer thickness in the FePt/Ag bilayer films, in particular, not only affect the disorder-order transition temperature [26] and the structural order of $L1_0$-fct phase [27], but also can affect the coercivity [28, 29], perpendicular anisotropy [30], and the FePt-Ag nanoparticles orientation [31]. In the present work, we grew and annealed the FePt granular nanolayers in the presence of Ag and have shown that in the presence of Ag, as in the presence of Cu, the c lattice constant of fct-FePt decreases. For this purpose, we have used indirect exchange interaction (RKKY) between magnetic atoms. We, additionally, have investigated the effect of Ag presence on the FePt nanoparticles orientation and coercivity during FePt-Ag nanostructure formation by annealing.

2 experimental details

Fe, Pt, and Ag were deposited by sputtering system (DST3-A model) on single crystals of Si (001) substrates by DC (for Ag) and RF (for Fe and Pt) at 500°C. The substrates, before the sputtering, were cleaned in ultrasonic system by acetone. The depositions were carried out at the base pressure of 10^{-5} Torr, Ar atmosphere of 10^{-2} Torr, DC voltage and RF power of 243 V and 74 W, respectively. The deposition rate of films in co-sputtering was selected 0.1 Å/s for Ag and 0.9 Å/s for FePt, respectively. The rate was determined by a quartz crystal oscillator. Some of the samples, then, were annealed in 90% Ar + 10% H_2 atmosphere for 60 min. The Fe to Pt atomic percentage ratio in all samples is equal to $Fe_{35}Pt_{65}$. In Table 1, the sputtering and annealing conditions are listed.

Table 1: The sputtering and annealing conditions.

Sample	1	2	3
Kind of nanostructure	FePt	FePt	FePt / Ag
Substrate temperature (°C)	500	500	R.T.
Annealing temperature (°C)	-----	600	500
Thickness (nm)	20	20	20/40
Rate of deposition (Å/s)	2	2	0.5/4.5
Sample	4	5	6
Kind of nanostructure	FePt-Ag / Ag	FePtAg-Ag	FePt-Ag
Substrate temperature (°C)	R.T.	500	500
Annealing temperature (°C)	600	-----	550
Thickness (nm)	20/40	10	10
Rate of deposition (Å/s)	0.5/4.5	1	1

In samples (1) and (2), Fe and Pt have been co-sputtered on the Si substrate at 500°C. Then, sample (2) has been annealed in the oven for 60 min. First, a layer of Ag in samples (3) and (4) are grown on Si, and in the second step, Fe and Pt have been co-sputtered at room temperature. In the third step, samples (3) and (4) have been annealed at 500°C and 600°C in the oven for 60 min, respectively. As a result, sample (4) has been converted to the nanostructure of FePt-Ag on the Ag layer. In samples (5) and (6), three kinds of metals, namely, Fe, Pt, and Ag have been co-sputtered on the Si substrate at 500°C, and in the second step, sample (6) has been annealed in the oven at 550°C for 60 min;

consequently, high temperature has led to the FePt-Ag nanostructure formation.

The crystal structures of samples were characterized by X-ray diffraction (XRD), STOE STADI MP model with Cu (k_α) radiation and wave length of $\lambda = 1.5406$ Å. The magnetic properties and hysteresis curves were measured by vibrating sample magnetometer (VSM), Lake-Shore model 7400 with the maximum field up to 20 kOe, at room temperature. The size and the surface distribution of grains were observed by field emission scanning electron microscopy (FE-SEM) and the composition of films were determined by using the energy dispersive X-ray spectroscopy (EDX), model MIRA3 Tescan working at 15.0 kV.

3 Results and Discussion

Figure 1 shows the FE-SEM images of samples 1-6. In Fig. 1a, as it can be seen, the FePt grains in the absence of annealing are single-sized and approximately 15 nm in size. However, after annealing, their sizes have been increased (Fig. 1b). The FePt grains in Fig. 1c have been settled on the thin layer of Ag (FePt /Ag), then, the sample has been annealed at 500°C. Figure 1d shows that besides larger FePt grains, other nanoparticles with the size of smaller than 20 nm have been also formed at 600°C. With increasing of temperature from 500°C to 600°C, two types of change occur in the nanostructure of the sample: a) The size of FePt nanoparticles increases from 20 nm to approximately 40 nm; b) Ag nanoparticles are formed with the size of less than 20 nm. The mechanism of smaller Ag nanoparticles formation in higher temperature, which has been shown in Fig. 1d, is as follows: In the FePt/Ag/Si system at 600°C, some of the Ag atoms separate from the middle layer of Ag and enter the FePt crystal lattice, but because of instability, they finally form a separate crystal lattice with Ag tiny grains. In fact, the formation of new smaller nanoparticles in higher temperatures is due to the temporary formation of unstable FePtAg compound as well as recrystallization of Ag in the form of separated nanoparticles which makes the FePt-Ag nanostructure.

The effect of fabrication methods and their differences is as follows: In the co-sputtering process, Ag atoms with a partial percentage are gradually lain in the crystal lattice; this provides the possibility of the FePtAg-Ag formation (Fig. 1e), but in the annealing stage, Ag atoms coalescence and form separate nanocrystals, leading to FePt-Ag nanostructure (Fig. 1f). This result is also determined by XRD pattern of sample 6. Although the FePt grains in sample (1) have a better nanostructure in the absence of annealing, but the annealing process in the presence of Ag causes the crystalline orientation of the nanoparticles. This effect is discussed in XRD and VSM results. In Figs. (1g and 1h) the middle layer is Ag; due to being in the oven, the thickness of the layers has increased.

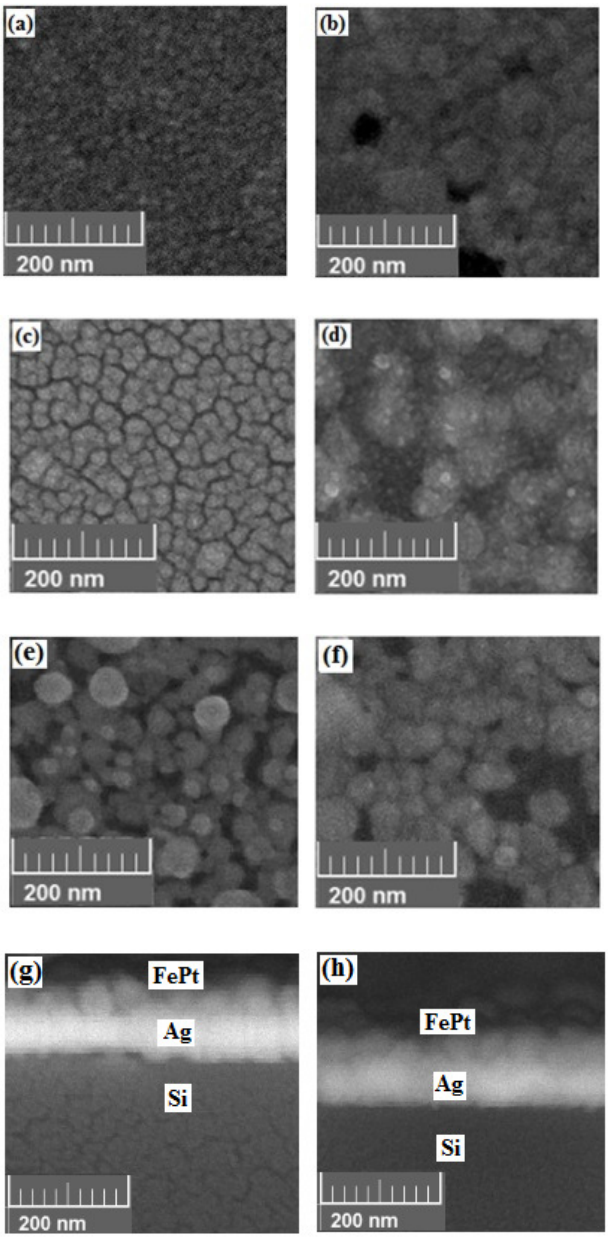

Figure 1. FE-SEM images of samples 1-6. a) FePt, b) FePt annealed at 600°C, c) FePt / Ag, d) FePt-Ag / Ag, e) FePtAg-Ag, f) FePt-Ag. Panels g and h show the cross-section of samples (3) and (4), respectively.

Figure 2 shows the pattern of X-ray diffraction of samples 1-6. Figure 2a is the XRD pattern of FePt nanoparticles before the $L1_0$ phase transition. The XRD peak in this figure is wider and indicative of the smaller size of the grains in sample (1), which has been also shown in Fig. 1a. The obtained size for the grains, through XRD and FE-SEM analyses, is 16.8 nm and 15 nm, respectively. In Fig. 2b the appearance of low intensity (001) and (110) peaks at $2\theta = 24°$ and 33°, respectively, shows $L1_0$ –FePt compound ordering phase. These two peaks, without Ag are weak even after annealing (sample 2). In the sample (3) the sublayer of Ag contributes to the $L1_0$ phase transition by annealing at 500°C and the appearance of (001) and (110) peaks (Fig. 2c). In sample (4), that has been annealed at 600°C, the further separation of the two (200) and (002) peaks from each other (Fig. 2d) and the increase in (001) peak intensity indicate that the $L1_0$ phase has been well formed in the FePt nanoparticles. The intensity of (001) peak, furthermore, has approached the intensity of (111) peak and the intensity of (002) peak has become larger than that of (200) peak in Fig. 2d. These are also evidence for another order construction, which is called crystal orientation, where easy axes of nanoparticles (c-axes) are aligned in the same direction to some extent.

In fact, the Ag atoms were separated from their underneath layer at 600°C. We have presented the effect of Ag on the formation of the FePt structure with $L1_0$-FePt compound ordering in [32]. The reason why and how $L1_0$-FePt compounds are formed at lower temperatures through Ag presence is that solitary Ag atoms lie in the FePt lattice, but with increasing their number, coalescing to each other and part of them exit from the lattice in order to form Ag nanocrystals. Consequently, their empty places in the FePt crystal structure contribute to the mobility of Fe and Pt atoms to form the new $L1_0$-FePt structure [33], resulting in a phase transition at lower temperatures [26]. Overall, Ag atoms account for two mechanisms in order to coalescence to each other and form Ag grains:

a) Exiting from FePt crystal lattice and forming separate Ag grains; this leads to the decrease in $L1_0$-FePt transition temperature so that the (001) and (110) peaks appear and the separation of (200) and (002) peaks from each other are the signs of this new phase.

b) Making FePt nanoparticles with a low percentage of Ag to align crystalline adjust to each other; this leads to the increase in the (001) peak intensity (Fig. 2d).

The (001) peak in the XRD pattern of sample (5) has been formed in $2\theta = 25°$ (Fig. 2e). The compound of this sample, which has been deposited on the Si (001) hot substrate at 500°C, is $Fe_{31}Pt_{58}Ag_{11}$ based on the EDX results (Fig. 3). The Ag and FePt co-sputtering in the short deposition time, with respect to the annealing time in the oven, has caused partial of Ag atoms to remain in the FePt crystal lattice and affected indirect exchange interaction inside the nanoparticles (RKKY) [6- 8]. This is because Ag free electrons increase the effective value of the Fermi wave vector (k_F) which leads to a smaller lattice constant. The shift of (001) peak from 24° in sample 3 (Fig. 2c) to 25° in sample 5 (Fig. 2e) is the evidence for this effect. To confirm this issue, we can compare sample (6) with sample (5), see Figs. 2f and 2e. Sample (6) is the same as sample (5), but it was annealed in the oven at 550°C for 1 hour. In fact, the annealing process causes Ag atoms to exit from the FePt nanoparticles crystal lattice and the (001) peak is formed in $2\theta = 24°$ (Fig. 2f). The appeared peak in $2\theta = 25°$ with lower intensity is the result of the type of FePt nanoparticles in which the Ag atoms remain. The FePt lattice constant (c) in sample (4) and the FePtAg lattice constant (c) in sample (5), that are obtained from (001) peak, are 3.70 Å and 3.56 Å, respectively. Indeed, the variation of FePt crystal lattice constant is due to:

(a) In the $L1_0$-FePt structure, the Pt paramagnetic metal atoms, with lying among the Fe magnetic atoms in the c direction, lead to the indirect exchange interaction (RKKY) and decrease the (c) with respect to the (a) lattice constant. The maximum of exchange constant (J) in this interaction is where the distance of the two magnetic atoms are proportional to $1/2k_F$ [8, 34], where k_F is the paramagnetic metal Fermi surface radius, that has been lain among magnetic atoms.

(b) The presence of Ag free electrons leads to increasing of the effective value of the Fermi wave vector (k_F) and decreasing of the distance of Fe magnetic atoms in the c direction inside of the FePt nanoparticles, which further reduces the lattice constant in the same direction. This also can be explained by RKKY interaction inside the nanoparticles. The shift of (001) peak from $2\theta = 24°$ to $2\theta = 25°$ is an experimental evidence for the effect of Ag in FePtAg.

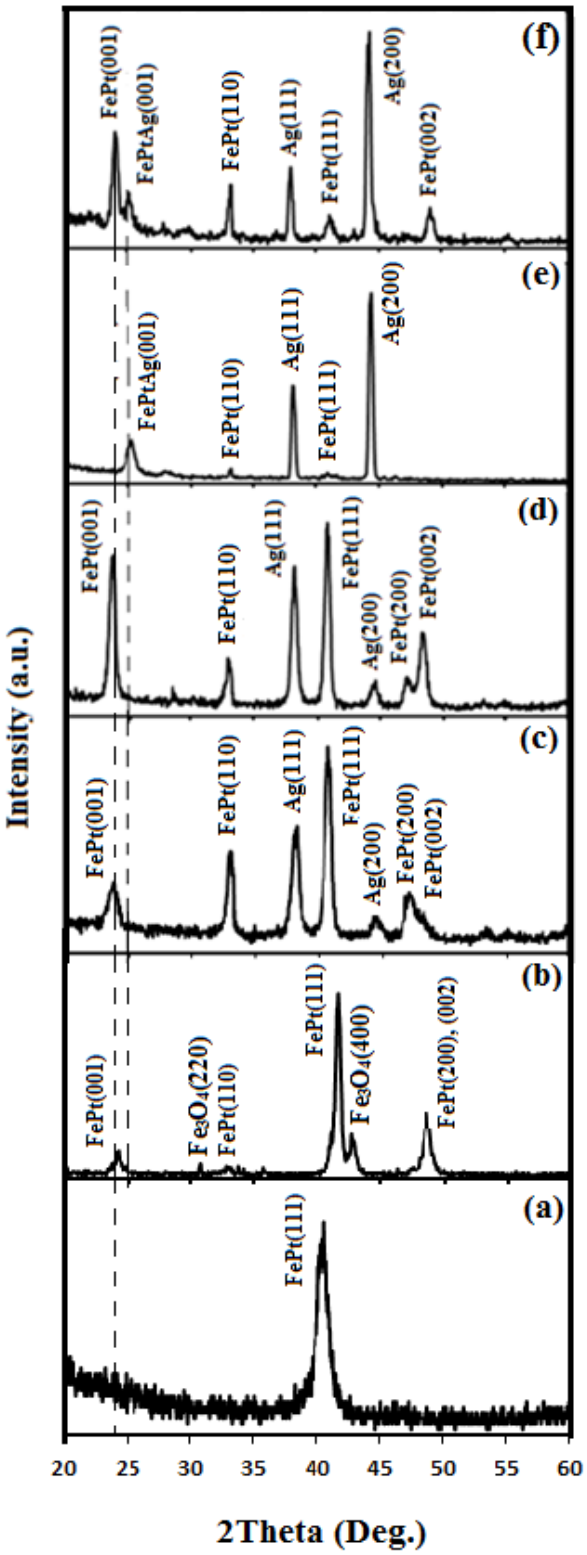

Figure 2. XRD patterns of samples 1-6. a) FePt without compound ordering, b) FePt with slight compound ordering, c) FePt / Ag with compound ordering, d) FePt-Ag / Ag with compound ordering and oriented, e) FePtAg-Ag with reducing of lattice constant, f) FePt-Ag with (001) peak duality after annealing.

(c) The result of RKKY interaction calculation in comparison with the result of XRD analysis is as

$n_{Pt} / (n_{Pt} + n_{Ag}) = 58 / (58 + 11) = 0.84$, where n_{Pt} and n_{Ag} are Pt and Ag atomic ratios, respectively.

The result of RKKY interaction is: $c_{FePtAg} / c_{FePt} = (k_F)_{FePt} / (k_F)_{FePtAg} = (0.84)^{1/3} = 0.94$

The result of XRD analysis is: $c_{FePtAg} / c_{FePt} = 3.56 / 3.70 = 0.96$, and this is an experimental confirmation of RKKY exchange interaction model.

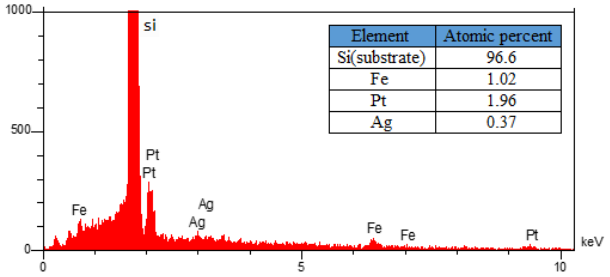

Figure 3. EDX analysis for the compound of Fe31Pt58Ag11.

The results of magnetic analysis (VSM) of sample (4), which has been shown in Fig. 4, indicates that the phase transition has occurred, and FePt ferromagnetic nanocrystals have been partially oriented. The coercivety in the easy direction, that is normal to the surface (Fig. 4a), and the hard direction, that is parallel to the surface (Fig. 4b), are 0.85 T and 0.75 T, respectively. Furthermore, the remnant magnetization (M/M_S) in the easy direction approaches to 1 and in the hard direction is 0.5. The privilege of Ag over Cu for adding to FePt is that, Ag increases the coercivety (H_C), but Cu [18] decreases it.

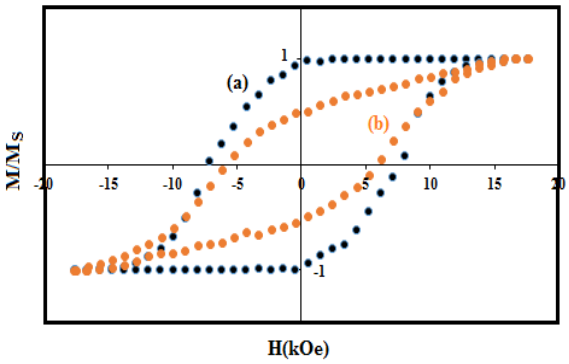

Figure 4. Curve (a) out-of-plane and curve (b) in-plane hysteresis loops of sample (4). The high coercivity is due to the uniaxial magnetocrystalline anisotropy of $L1_0$-fct phase in the Fe-Pt compound.

4 Conclusions

The impacts of Ag presence on $L1_0$-FePt nanoparticles are as follows:

a) Reducing the transition temperature; the symptom of this is the appearance of (001) and (110) peaks of $L1_0$-FePt structure, according to Fig. 2c.

b) Making $L1_0$-FePt nanoparticles crystalline directional, the signs increas in (001) to (111) and (002) to (200) peaks intensity ratios [I(001)/I(111), I(002)/I(200)] and difference of M(H) loops in two directions.

c) The annealing process in the presence of Ag gives rise to the formation of FePt-Ag/Ag nanostructure, according to Fig. 1d.

d) Reduction in the c lattice parameter of FePtAg; the symptom of this is the shift of (001) peak from $2\theta = 24°$ to $2\theta = 25°$ before annealing process, Fig. 2e.

e) Ag free electrons, inside nanoparticles, decrease the distance of Fe atoms in the c direction of crystal lattice. This is the result of decreasing the equilibrium distance of magnetic atoms in the RKKY exchange interaction, because the Ag free electrons increase the effective value of the Fermi surface radius (k_F). Therefore, the change of the lattice constant (c) can appear in the (001) peak shift.

References

[1] S. Bahamida, A. Fnidiki, M. Coisson, G. Barrera, F. Celegato, E. S. Olivetti, P. Tiberto, A. Laggoun, M. Boudissa, "Effect of the A1 to $L1_0$ transformation on the structure and magnetic properties of polycrystalline $Fe_{56}Pd_{44}$ alloy thin films produced by thermal evaporation technique." Thin Solid Films, **668** (2018) 9.

[2] P. Ravindran, A. Kjekshus, H. Fjellvag, P. James, L. Nordstrom, B. Johansson, O. Eriksson, "Large magnetocrystalline anisotropy in bilayer transition metal phases from first-principles full-potential calculations." Physical Review B, **63** (2001) 144409.

[3] S. A. Khan, P. Blaha, H. Ebert, J. Minar, O. Sipr, "Magnetocrystalline anisotropy of FePt: A detailed view." Physical Review B, **94** (2016) 144436.

[4] T. Burkert, O. Eriksson, S. I. Simak, A. V. Ruban, B. Sanyal, L. Nordstrom, J. M. Wills, "Magnetic anisotropy of $L1_0$ FePt and $Fe_{1-x}Mn_xPt$." Physical Review B, **71** (2005) 134411.

[5] O. N. Mryasov, "Magnetic interactions and phase transformations in FeM, M = (Pt, Rh) ordered alloys." Phase Transitions, **78** (2005) 197.

[6] M. D. Stiles, "Interlayer exchange coupling." Journal of Magnetism and Magnetic Materials, **200** (1999) 322.

[7] P. Wahl, P. Simon, L.Diekhoner, V. S. Stepanyuk, P. Bruno, M. A. Schneider, K. Kern, "Exchange interaction between single magnetic adatoms." Physical Review Letters, **98** (2007) 056601.

[8] J. Wiebe, L. Zhou, R. Wiesendanger, "Atomic magnetism revealed by spin-resolved scanning tunnelling spectroscopy." Journal of Physics D: Applied Physics, **44** (2011) 464009.

[9] D. A. Gilbert, L. W. Wang, T. J. Klemmer, J. U. Thiele, C. H. Lai, K. Liu, "Tuning magnetic anisotropy in (001) oriented $L1_0$ $(Fe_{1-x}Cu_x)_{55}Pt_{45}$ films." Applied Physics Letters, **102** (2013) 132406.

[10] G. Varvaro, S. Laureti, D. Fiorani, "$L1_0$ FePt-based thin films for future perpendicular magnetic recording media." Journal of Magnetism and Magnetic Materials, **368** (2014) 415.

[11] M. Ohtake, M. Nakamura, M. Futamoto, F. Kirino, N. Inaba, "Enhancement of $L1_0$ ordering with the c-axis perpendicular to the substrate in FePt alloy film by using an epitaxial cap-layer." AIP ADVANCES, **7** (2017) 056320.

[12] S. Singh, C. L. Prajapat, M. Gupta, S. Basu, "Room temperature superparamagnetism in ternary $(Fe_{50}Pt_{50})_{0.42}Cu_{0.58}$ phase at interfaces on annealing of $Fe_{50}Pt_{50}$/Cu multilayer." Journal of Magnetism and Magnetic Materials, **462** (2018) 58.

[13] Y. C. Lai, Y. H. Chang, Y. C. Chen, C. H. Liang, "Inductive magnetization of low-temperature ordered $L1_0$-FePt with CoAg underlayer." Journal of Applied Physics, **101** (2007) 053913.

[14] R. Moradi, S. A. Sebt, H. K. Maleh, R. Sadeghi, F. Karimi, A. Bahari, H. Arabi, "Synthesis and application of FePt/CNTs nanocomposite as a sensor and novel amide ligand as a mediator for simultaneous determination of glutathione, nicotinamide adenine dinucleotide and tryptophan." Physical Chemistry Chemical Physics, **15** (2013) 5888.

[15] S. A. Sebt, H. Ashourifar, M. M. Larijani, "The effect of electron flow on FePt nanoparticles under heat treatment." Physica Scripta, **85** (2012) 055804.

[16] S. A. Sebt, A. Bakhshayeshi, M. R. Abolhassani, "Magnetic properties of core / shell nanoparticles with magnetic or nonmagnetic shells." Journal of Statistical Mechanics: Theory and Experiment, **2012** (2012) P09006.

[17] S. Jain, C. Papusoi, R. Admana, H. Yuan, R. Acharya, "Magnetization reversal process and evaluation of thermal stability factor in Cu doped granular $L1_0$ FePt films." Journal of Applied Physics, **123** (2018) 193902.

[18] C. Brombacher, H. Schletter, M. Daniel, P. Matthes, N. Johrmann, M. Maret, D. Makarov, M. Hietschold, M. Albrecht, "FePtCu alloy thin films: Morphology, $L1_0$ chemical ordering, and perpendicular magnetic anisotropy." Journal of Applied Physics, **112** (2012) 073912.

[19] K. Sharma, G. Sharma, M. Gupta, V. R. Reddy, A. Gupta, "Enhancement of $L1_0$ transformation in Fe/Pt multilayer by Cu addition." AIP ADVANCES, **8** (2018) 105118.

[20] M. Maret, C. Brombacher, P. Matthes, D. Makarov, N. Boudet, M. Albrecht, "Anomalous x-ray diffraction measurements of long-range order in (001) - textured $L1_0$ FePtCu thin films." Physical Review B, **86** (2012) 024204.

[21] Y. Liu, Y. Jiang, N. Kadasala, X. Zhang, C. Mao, Y. Wang, H. Liu, Y. Liu, J. Yang, Y. Yan, "Effects of Au content on the structure and magnetic properties of $L1_0$-FePt nanoparticles synthesized by the sol-gel method." Journal of Solid State Chemistry, **215** (2014) 167-170.

[22] I. A. Vladymyrskyi, A. E. Gafarov, A. P. Burmak, S. I. Sidorenko, G. L. Katona, N. Y. Safonova, F. Ganss, G. Beddies, M. Albrecht, Y. N. Makogon, D. L. Beke, "Low-temperature formation of the FePt phase in the presence of an intermediate Au layer in Pt/Au/Fe thin films." Journal of Physics D: Applied Physics, **49** (2016) 035003.

[23] V. Deepchand, F. M. Abel, V. Tzitzios and G. C. Hadjipanayis, "Chemical synthesis of $L1_0$ Fe-Pt-Ni alloy nanoparticles." AIP ADVANCES, **8** (2018) 056210.

[24] C. H. Lai and C. H. Ho, "Improvement of magnetic properties of FePt nanoparticles by adding Mn." Journal of Applied Physics, **97** (2005) 10J314.

[25] D. B. Xu, J. S. Chen, T. J. Zhou, G. M. Chow, "Effects of Mn doping on temperature-dependent magnetic properties of $L1_0$ FeMnPt." Journal of Applied Physics, **109** (2011) 07B747.

[26] S. S. Kang, D. E. Nikles, J. W. Harrell, "Synthesis, chemical ordering, and magnetic properties of self-assembled FePt-Ag nanoparticles." Journal of Applied Physics, **93** (2003) 7178.

[27] Y. Zhang, W. Yu, F. Chen, M. Liu, Y. Yu, H. Li, "Effect of Ag underlayer thickness on the microstructure and magnetic properties of $L1_0$-FePt films." Applied Physics A, **110** (2013) 249.

[28] C. Y. You, Y. K. Takahashi, K. Hono, "Particulate structure of FePt thin films enhanced by Au and Ag alloying." Journal of Applied Physics, **100** (2006) 056105.

[29] B. S. D. C. S. Varaprasad, Y. K. Takahashi, J. Wang, T. Ina, T. Nakamura, W. Ueno, K. Nitta, T. Uruga, K. Hono, "Mechanism of coercivity enhancement by Ag addition in FePt-C granular films for heat assisted magnetic recording media." Applied Physics Letters, **104** (2014) 222403.

[30] Y. Tokuoka, Y. Seto, T. Kato, S. Iwata, "Effect of Ag addition to $L1_0$ FePt and $L1_0$ FePd films grown by molecular beam epitaxy." Journal of Applied Physics, **115** (2014) 17B716.

[31] R. Roghani, S. A. Sebt, A. Khajehnezhad, "The texture ordering in $L1_0$-FePt-Ag nanocomposites." Journal of Theoretical and Applied Physics, **14** (2020) 47.

[32] R. Roghani, S. A. Sebt, A. Khajehnezhad, "High magnetic coercivity of FePt-Ag/MgO granular nanolayers." Physica C: Superconductivity and its applications, **549** (2018) 15.

[33] H. Wang, P. Shang, J. Zhang, M. Guo, Y. Mu, Q. Li, H. Wang, "One-step synthesis of high-coercivity $L1_0$-FePtAg nanoparticles: Effects of Ag on the morphology and chemical ordering of FePt nanoparticles." Chemistry of Materials, **25** (2013) 2450.

[34] J. M. D. COEY: Magnetism and Magnetic Materials, Cambridge University Press, New York, 2010.